NATIONAL ADVISORY COMMITTEE FOR AERONAUTICS

WARTIME REPORT

ORIGINALLY ISSUED

July 1945 as
Restricted Bulletin L5F15

THEORETICAL AND EXPERIMENTAL DYNAMIC LOADS

FOR A PRISMATIC FLOAT HAVING AN

ANGLE OF DEAD RISE OF $22\frac{1}{2}^{\circ}$

By Wilbur L. Mayo

Langley Memorial Aeronautical Laboratory
Langley Field, Va.

NACA

WASHINGTON

NATIONAL ADVISORY COMMITTEE FOR AERONAUTICS

RESTRICTED BULLETIN

THEORETICAL AND EXPERIMENTAL DYNAMIC LOADS

FOR A PRISMATIC FLOAT HAVING AN

ANGLE OF DEAD RISE OF $22\frac{1}{2}°$

By Wilbur L. Mayo

SUMMARY

An application of a modified hydrodynamic impact theory is presented. Plots are given from which the maximum load, the time to reach maximum load, and the variation of load with time may be obtained for a prismatic float of $22\frac{1}{2}°$ angle of dead rise for different combinations of flight-path angle, trim, weight, velocity, and fluid density. The curves cover the range of trim, flight-path angle, and weight-velocity relationship for conventional airplanes. Test data obtained in the Langley impact basin are presented and are used to establish the validity of the theoretical curves.

INTRODUCTION

During the past 15 years numerous reports have been written on hydrodynamic theory for the landing impact of seaplane floats but none of these treatments has been accepted for design purposes. An analysis (unpublished) of available treatments (references 1 to 8) was undertaken by the Langley Laboratory in order to determine the validity and possibilities of the theory. This analysis showed that the previous treatments did not properly take into account certain hydrodynamic forces, particularly those associated with planing action.

An application of a modified hydrodynamic impact theory is presented herein for the case of a rigid prismatic float having an angle of dead rise of $22\frac{1}{2}°$. The validity of this theory is established experimentally by

comparison with data for a rigid float tested in the
Langley impact basin. The theoretical solutions are
directly applicable to the calculation of the dynamic
response of elastic airframes, if it is assumed that the
variation of load with time is not substantially affected
by the structural elasticity of the body. Experimental
verification of the rigid-body equations is significant
in that it establishes the validity of a basic hydro-
dynamic theory which is equally applicable to the deri-
vation of equations that involve modification of the force
history due to structural elasticity. Additional work is
planned to include the effect of the structural response
on the loading function.

A large number of force histories is given by three
plots from which the maximum load, the time to reach maxi-
mum load, and the variation of load with time may be
obtained. The equations used in obtaining the results are
given and the method of solution is explained in an
appendix.

SYMBOLS

β angle of dead rise, degrees

τ trim, degrees

γ flight-path angle, degrees

W weight of float

V resultant velocity at instant of first contact
            with water surface

ρ mass density of fluid

g acceleration of gravity

$t_{a_{max}}$ elapsed time between instant of first contact with
            water surface and instant of maximum acceleration

m mass of float

$ni_{W_{max}}$ impact load factor (maximum hydrodynamic load
            normal to water surface divided by W)

Where units are not given, any consistent system of units may be used.

RESULTS

Comparison of Theory and Experiment

Theoretical solutions made for a rigid prismatic float having an angle of dead rise of $22\frac{1}{2}^{\circ}$ were compared with data obtained from tests of a float having the form of the forebody shown in figure 1 and the offsets given in table I. The agreement obtained in this comparison indicates that the theory can be applied to floats which do not differ from a prism more than the float in figure 1. Figure 2 shows the variation of the impact-load-factor coefficient with flight-path angle for trims ranging from 3° to 12°. The equations, from which the curves were obtained, were derived on the assumption that the ratios of fluid compressibility, viscous forces, and gravity forces to inertia forces are negligible. In tank tests of seaplanes the ratio of the gravity forces to the inertia forces (Froude's number) is the criterion for determining the similarity of the flow for similar hulls of different size. The high speed associated with an impact tends to increase the inertia forces and to decrease the relative importance of the gravity forces; however, the tendency to design large airplanes to have landing speeds of the same order as small airplanes results in lesser acceleration for the larger weights and greater importance of the gravity forces. For a specific landing speed there is a weight range above which the gravity forces may be of substantial importance.

Experimental data are included in figure 2 for the two boundary values of trim investigated. The data were obtained at widely different speeds for a float weighing 1100 pounds. Even the points obtained in low-speed tests, for which gravity forces are of greater importance than for high-speed tests, show remarkable agreement with computations made on the assumption that the gravity forces are negligible. For a full-scale landing speed of 70 miles per hour the experimental data represent airplanes weighing up to 160,000 pounds. For higher landing speeds, such as may occur with military airplanes, the represented weight is even greater. These interpretations of the experimental check show that the theoretical computations presented

herein will give good results for all present-day air-
planes. Pertinent data with regard to the weight-velocity
relationships for equal ratios of the gravity forces to
the inertia forces $\left(\text{equivalent values of } V\left(\dfrac{\rho}{g^2 W}\right)^{1/6}\right)$ are
included in figure 2.

The fact that the curves in figure 2 intersect shows
that the variation of maximum impact force with trim for
large flight-path angles is the reverse of the variation
for small flight-path angles. For small flight-path angles
the planing forces predominate and, since the effect of
increased trim is to increase the downwash angle of the
deflected stream, the resulting increase of the resultant
force for a specific draft at the step causes the impact
to be more severe than for small trim. For large flight-
path angles the increase of the virtual mass due to verti-
cal velocity dominates the impact force and, since the
effect of increased trim is to lower the rate of increase
of the virtual mass for a specific vertical velocity,
lesser force for a specific draft, and consequently a
less severe impact than for small trim, occurs.

Figure 3 shows the variation of the time to reach
maximum acceleration with flight-path angle for trims
ranging from 3° to 12°. The plot is similar to figure 2
and therefore does not require further explanation.

Figure 4 is a plot of acceleration ratio against time
ratio for a wide range of flight-path angle and trim. The
ratios are based on the acceleration and time at any
instant as compared with the maximum acceleration and the
time to reach maximum acceleration. By interpolating
between the curves of figure 4 and using the amplitude and
time plots of figures 2 and 3 to define the maximum accel-
eration and the time to reach maximum acceleration, any
number of time histories within the range of investigated
conditions can be constructed.

Because individual curves would be difficult to dis-
tinguish if all the solutions of the equations given in
the appendix were plotted, some of the solutions have been
grouped and the boundary lines for each group plotted in
figure 4. The solutions that lie between the boundary
lines are tabulated in figure 4. Although an approximate
interpolation can be effected between the boundary lines
of figure 4, the spacing is close enough to permit the use
of a line centered between these boundaries for practical
solutions.

The equations used to obtain figures 2 to 4 assume
that the beam of the float is large enough to prevent the
chine from coming into firm contact with the water. If
the chine does come into contact with the water, a discon-
tinuity occurs in the impact process and the conditions
specified by the equations of this report for the time of
chine contact must be taken as the initial conditions for
a different equation for the case of immersed chines. It
is planned that a later program will deal with such
calculations.

Applicability to Flight Impact

The load values given herein are based on the assump-
tion that the chines do not become immersed; it should be
noted that early immersion of the chines can cause only
reduction of the maximum load and hence conservative load
values. The variation of the impact force with draft,
which was obtained in the course of solving the equations
of the appendix for the force-time variation, was used
to determine the effects of beam loading, flight-path
angle, and trim on chine immersion. A comparison of the
data obtained in this study with available data for a
number of different airplanes was made. It was indicated
that the beam loadings of conventional American seaplanes
and flying boats are sufficiently light to ensure that
maximum load values given herein will not be unduly con-
servative. Some German airplanes, and possibly some
American flying boats with wartime overload, have high
beam loadings, which may cause the immersion of the chines
to be significant for high trims and steep flight-path
angles.

For small angles of dead rise and for large trims the
theory requires a different formula. Since the exact
manner of the transformation from the condition requiring
one formula to the condition requiring another formula is
not known, the formulas of the appendix should not be
applied indiscriminately.

The equations presented are for the absence of pulled-
up bow. The bow of the float tested is representative of
the bow of an actual flying boat; agreement between the
data obtained and the theoretical computations for the
prismatic float indicates that the effect of the bow is
not important for the conditions investigated.

Both the experimental data and the theoretical cal-
culations are for fixed-trim impact and therefore do not
indicate the effect of angular rotation during impact.
Various design considerations tend to locate the center
of gravity relative to the center of water pressure so as
to minimize angular acceleration. Even when substantial
angular accelerations are reached, the time to reach peak
load is believed to be short enough and the average angu-
lar velocity small enough to keep large angular displace-
ment from being reached during this period.

The experimental data used in the present report were
obtained in tests of the float shown in figure 1 with the
afterbody removed. Although exact evaluation of the
effects of afterbody loads is not possible at this time,
various design considerations ensure that actual airplanes
will have sufficient depth of the step and reduced trim
at the afterbody to be effective in promoting the shielding,
at impact speed, of the afterbody by the forebody and in
causing thereby the loads on the afterbody to be of rela-
tively small importance.

The experimental data used herein were obtained with
a float attached to a coasting carriage having a mass
about three times the mass of the float. This condition
involves slight reduction of the speed during impact,
whereas in the theoretical computations a constant hori-
zontal speed is assumed. By observing the relative magni-
tudes of the vertical and horizontal accelerations and
velocities for an impact and applying the laws of velocity
dissipation, even in the case in which the float is
entirely free in the drag direction, the reduction in
horizontal speed during the impact can be seen to be of
small importance. By using different constants in the
equations of the appendix, the reduction in horizontal
speed can be incorporated; however, it is felt that the
gain would be too slight to warrant the additional com-
plication.

The curves of the present report are for smooth-water
impacts but they will give approximate results for rough-
water impacts if the flight-path angle and the trim are
defined relative to the wave surface rather than relative
to the horizontal.

The equations in the appendix are based on the assump-
tion that the float is weightless (1g wing lift). Devia-
tion of the wing lift of the actual airplane from 1g will
affect the experimental results but the effect will
probably not be very large.

CONCLUSIONS

Application of a modified hydrodynamic impact theory to a rigid prismatic float with angle of dead rise of $22\frac{1}{2}^{\circ}$ and an analysis of data made to determine the validity of the theory indicate the following conclusions:

1. The effect of trim on load for large flight-path angles is the reverse of that for small flight-path angles. This reversal is due to a change in the relative importance of the planing and impact forces and shows that both the forces must be considered.

2. The agreement between experiment and theory was good, and thus the theory was proved adequate for the conditions investigated.

3. Since hydrodynamic impact theory does not take into account the effect of the gravity forces on the fluid flow, the agreement of this theory with experiment for the range of weight-velocity relationships for landing impacts of present-day airplanes indicated that the effect of gravity on the flow pattern is not important in impacts of such airplanes.

4. Consideration of the factors involved in applying the theoretical curves to actual airplanes indicated that such applications will give good results.

Langley Memorial Aeronautical Laboratory
  National Advisory Committee for Aeronautics
    Langley Field, Va.

APPENDIX

MATHEMATICAL FORMULAS AND METHOD OF SOLUTION

The following formulas were used in computing the curves of this report:

$$y^3 = \frac{6m \sin\tau \cos^2\tau}{(A - B)C}\left[\left(\frac{\dfrac{\dot{y}}{\dot{y}_0}\tan\gamma + \dfrac{A\sin\tau\cos\tau}{A - B\sin^2\tau}}{\tan\gamma + \dfrac{A\sin\tau\cos\tau}{A - B\sin^2\tau}}\right)^{\frac{A\cot^2\tau}{A - B\sin^2\tau}}\left(\frac{\tan\gamma + \tan\tau}{\dfrac{\dot{y}}{\dot{y}_0}\tan\gamma + \tan\tau}\right)^{\csc^2\tau} - 1\right] \quad (1)$$

$$-\ddot{y} = 3Cy^2 \frac{\left(\dfrac{\dot{y}}{y} + \dot{y}_0\dfrac{\tan\tau}{\tan\gamma}\right)\left[\dot{y}\left(A - B\sin^2\tau\right) + \dfrac{A\dot{y}_0 \sin\tau\cos\tau}{\tan\gamma}\right]}{6m\sin\tau\cos^2\tau + (A - B)\,Cy^3} \quad (2)$$

In equations (1) and (2)

$$A = 0.75\pi\rho\left(\frac{\pi}{2\beta} - 1\right)^2 + 0.79\frac{\rho}{\tan\beta}$$

$$B = 0.79\frac{\rho}{\tan\beta}$$

$$C = 1 - \frac{\tan\tau}{2\tan\beta}$$

where β is measured in radians and

y draft of float at any instant

$\dot{y}_o$ vertical velocity at contact

$\dot{y}$ vertical velocity of float at any instant

$\ddot{y}$ vertical acceleration of float at any instant

    Formulas (1) and (2) are not applicable when y is negative, that is, after the float has rebounded from the water surface. These solutions, which can be readily obtained from equation (2), lie in the region where y is negative. Efforts to obtain a solution giving the displacement explicitly as a function of the time have not been successful and, consequently, the following procedure was used to calculate the curves presented herein:

    1. Substitute arbitrary values of $\dot{y}$ in equation (1) and solve for the corresponding values of y.

    2. Substitute corresponding values of $\dot{y}$ and y in equation (2) and calculate the corresponding values of $\ddot{y}$.

    3. Repeat process for values of $\dot{y}$ selected to define adequately the $\ddot{y}$-curves with a minimum number of points.

    4. Plot the variation of $1/\dot{y}$ with y. For each point on this curve the acceleration is known from the previous steps. The time for each combination of y, $\dot{y}$, and $\ddot{y}$ can be obtained by integrating the area beneath and to the left of a particular point on the curve showing the variation of $1/\dot{y}$ with y. Determine such time values for intervals that approximately define the acceleration-time curve. Repeat the process for such y

and $\dot{y}$ combinations as are of greatest help in defining
the more critical portions of this curve.

The accuracy of the outlined method is dependent upon
the number of points for which solutions are made in order
to fair the various curves. After a certain amount of
experience with these solutions, the accuracy of a specific
solution may be approximated by estimating possible errors
involved in fairing the curves through the limited number
of points. It has been found that after the constants for
equations (1) and (2) are computed curves giving the
relations between acceleration, velocity, and draft within
an accuracy of the order of 1 percent can be obtained by
one computer in 3 or 4 hours.

REFERENCES

1.   von Kármán, Th.: The Impact on Seaplane Floats
        during Landing. NACA TN No. 321, 1929.

2.   Pabst, Wilhelm: Theory of the Landing Impact of
        Seaplanes. NACA TM No. 580, 1930.

2.   Pabst, Wilhelm: Landing Impact of Seaplanes. NACA TM
        No. 624, 1931.

4.   Wagner, Herbert: Landing of Seaplanes. NACA TM
        No. 622, 1931.

5.   Wagner, Herbert: Über Stoss- und Gleitvorgänge an
        der Oberfläche von Flüssigkeiten. Z.f.a.M.M.,
        Bd. 12, Heft 4, Aug. 1932, pp. 193-215.

6.   Schmieden, C.: Über den Landestoss von
        Flugzeugschwimmern. Ing.-Archiv., Bd. X, Heft 1,
        Feb. 1939, pp. 1-13.

7.   Sydow, J.: Über den Einfluss von Federung und
        Kielung auf den Landestoss. Jahrb. 1938 der
        deutschen Luftfahrtforschung, R. Oldenbourg
        (Munich), pp. I 329 - I 338. (Available as
        British Air Ministry Translation No. 861.)

8.   Kreps, R. L.: Experimental Investigation of Impact
        in Landing on Water. NACA TM No. 1046, 1943.

TABLE I.- OFFSETS OF LANGLEY IMPACT BASIN FLOAT MODEL M-1 (SEE FIG. 1)

[All dimensions are in inches]

Station	Half-breadth		Height above datum line			Height above keel	
	Chine	Deck	Keel	Chine	Deck	Chine	Deck
0	0	0	21.99	21.99	29.01	0	7.02
2	2.01	1.45	15.45	21.80	29.58	6.35	14.13
5	4.70	3.05	11.99	23.26	30.22	11.27	18.23
9	7.60	4.58	8.95	23.19	30.92	14.24	21.97
14	10.17	5.93	6.44	21.20	31.50	14.76	25.06
21	12.81	7.25	4.16	18.35	31.93	14.19	27.77
29	15.09	8.15	2.55	15.60	32.00	13.05	29.45
38	16.36	8.74	1.44	13.14	→	11.70	30.56
47	18.04	8.94	.72	11.27		10.55	31.28
58	18.87	9.00	.22	9.63		9.41	31.78
72	19.33	→	.02	8.31		8.29	31.93
87.25	19.40		0	7.91		7.91	32.00
106.625	19.40		0	7.91		7.91	32.00
a120.75F	19.40		0	7.91		7.91	32.00
b120.75A	18.67	8.82	1.95	9.54		7.59	30.05
137	17.83	8.09	3.95	11.41		7.46	28.05
153	16.85	6.54	5.91	13.18		7.27	26.09
169	15.65	4.13	7.87	14.81		6.94	24.13
185	14.00		9.84	16.17		6.33	22.16
201	11.74		11.77	17.24		5.47	20.23
216	8.59		13.66	17.69		4.03	18.34

aForebody.
bAfterbody.

NATIONAL ADVISORY
COMMITTEE FOR AERONAUTICS
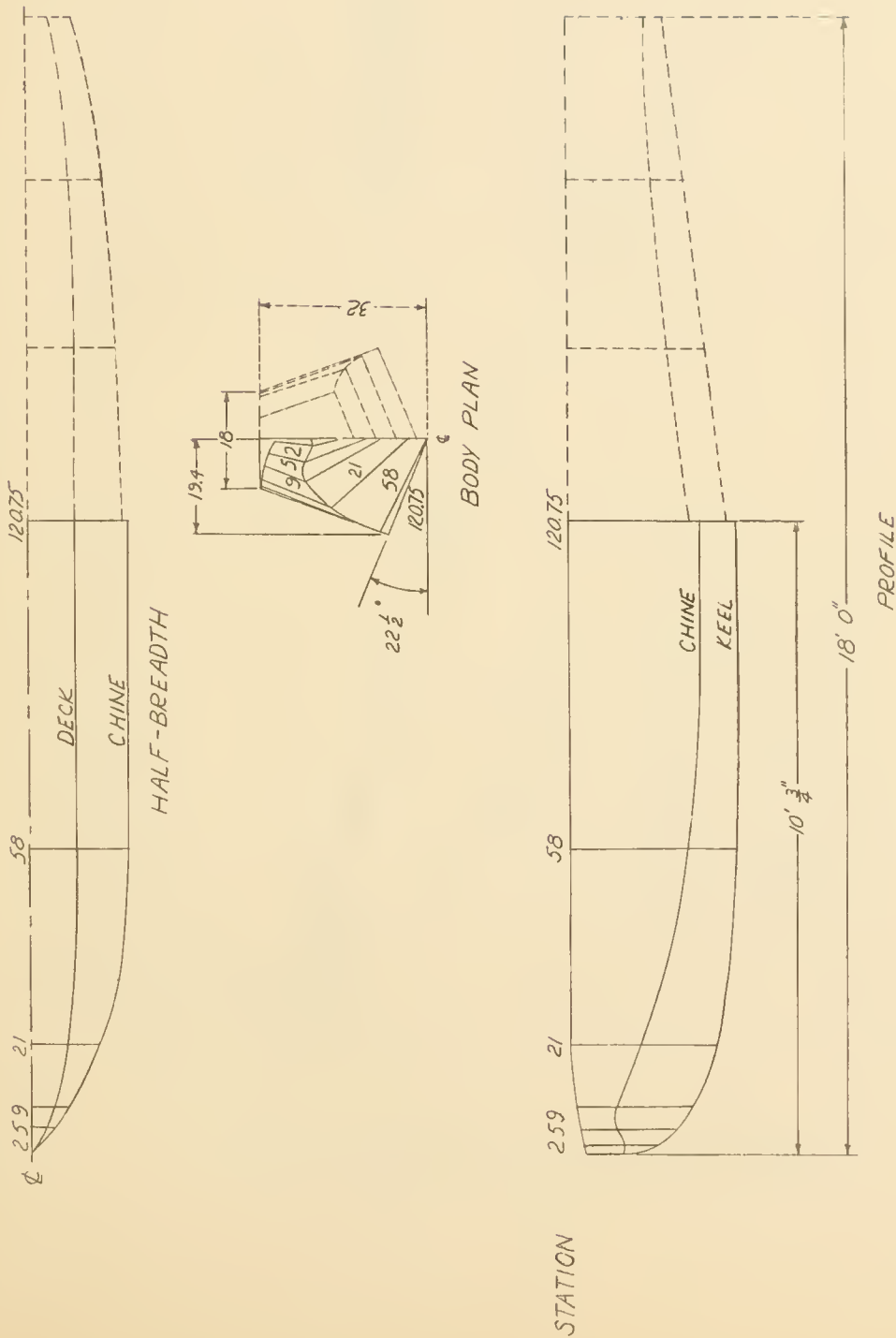
FIGURE 1.-LANGLEY IMPACT BASIN FLOAT MODEL M-1.
OFFSETS GIVEN IN TABLE I.

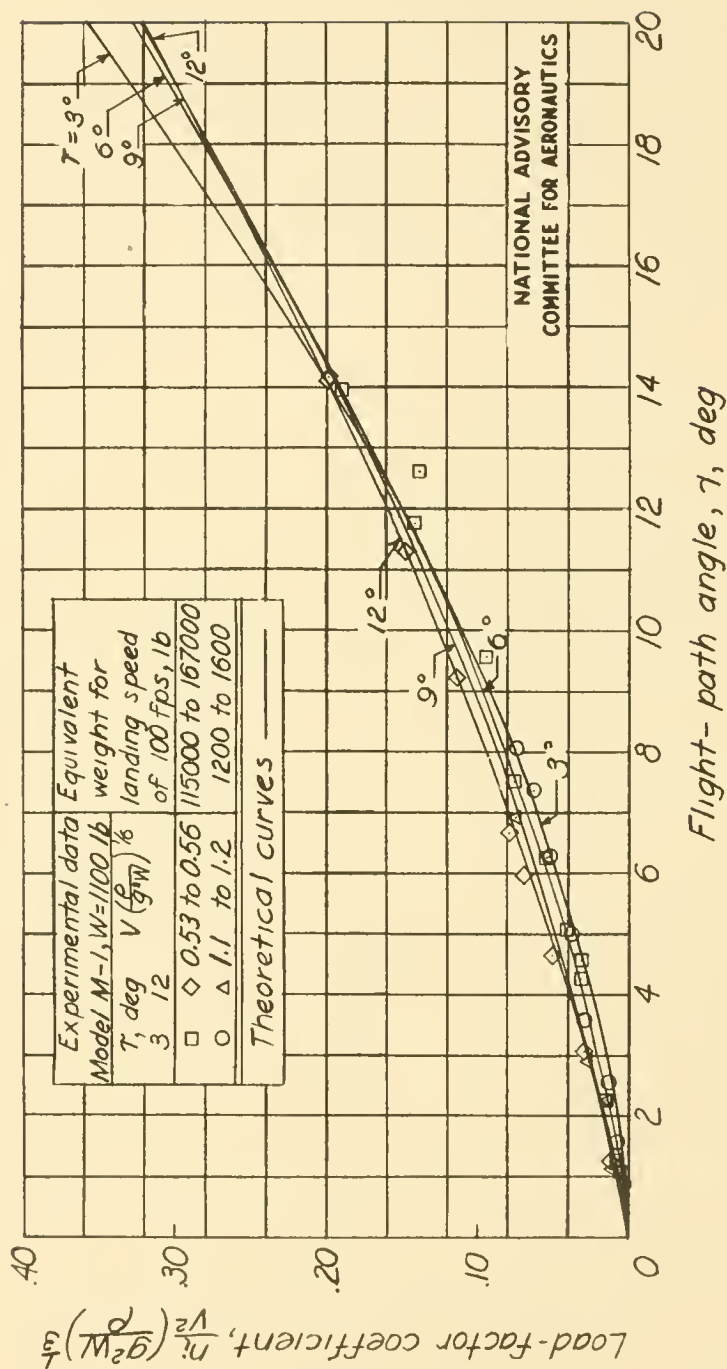Fig. 2   NACA RB No. L5F15

Figure 2.- Variation of load-factor coefficient with flight-path angle for a prismatic float having an angle of dead rise of $22\frac{1}{2}°$.

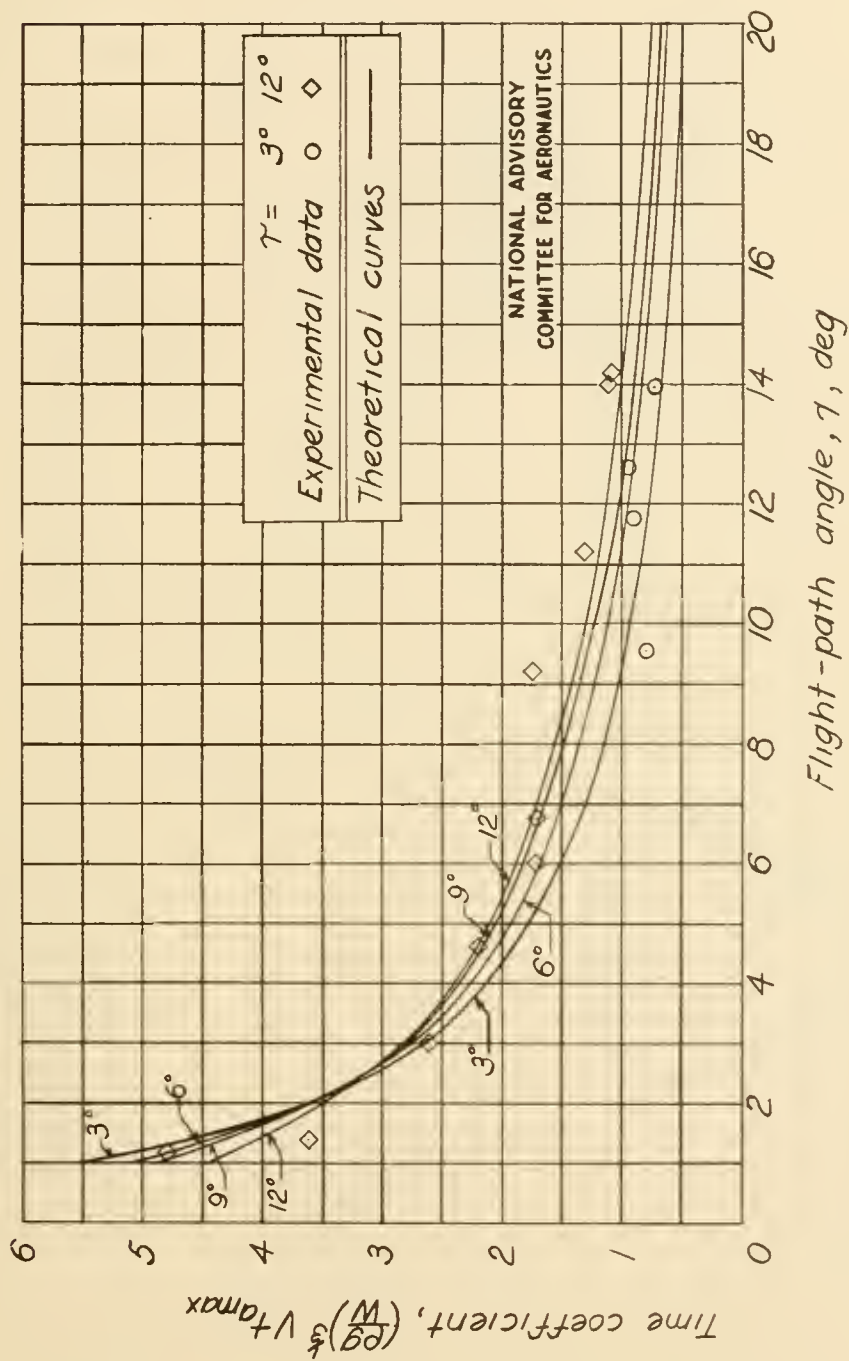Figure 3.- Variation of time coefficient with flight-path angle for a prismatic float having an angle of dead rise of $22\frac{1}{2}°$.

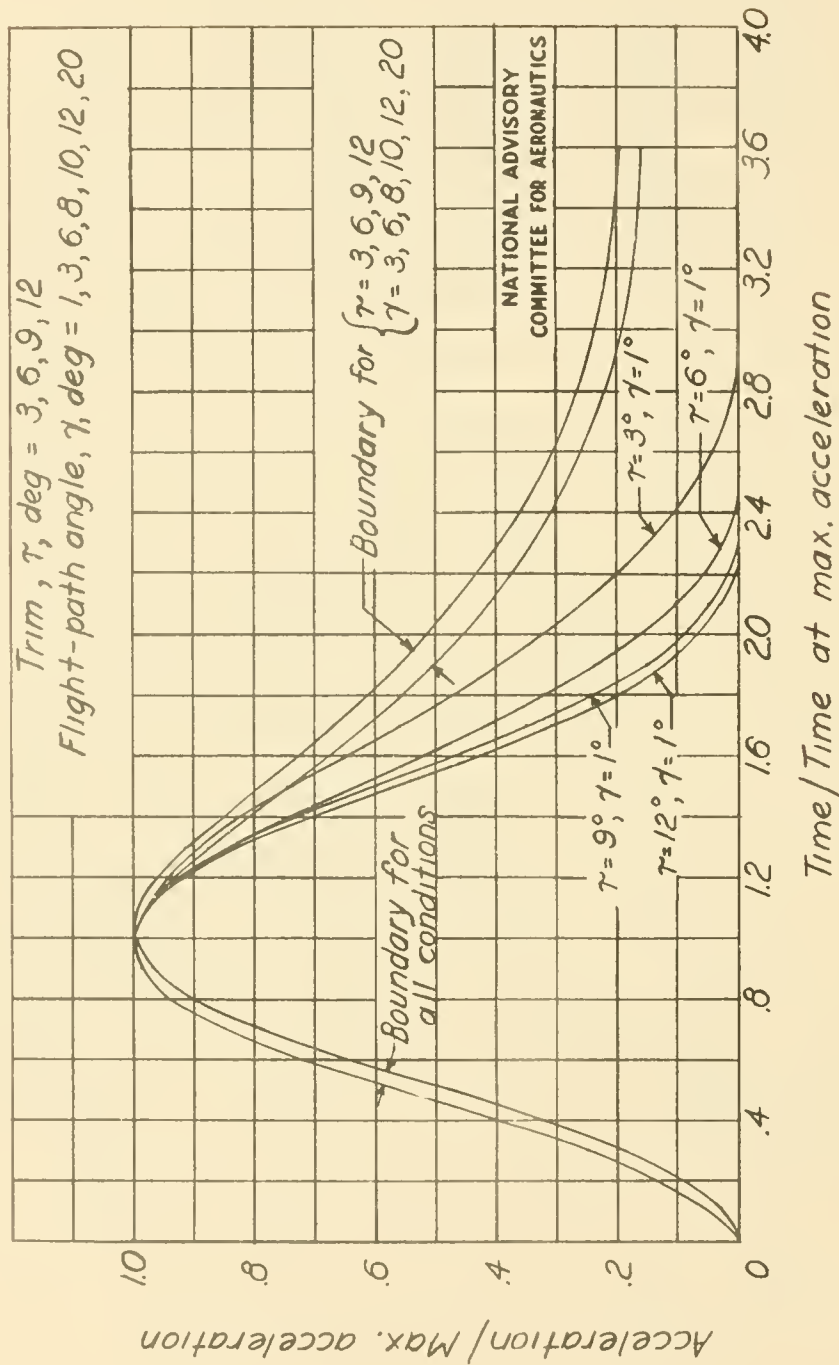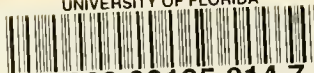Fig. 4   NACA RB No. L5F15

Figure 4.- Acceleration-time relation of impact for a prismatic float having an angle of dead rise of 22½° (computed).